

Analysis of pedestrian activity before and during COVID-19 lockdown, using webcam time-lapse from Cracow and machine learning.

Robert Szczepanek^{Corresp. 1}

¹ Faculty of Environmental and Power Engineering, Cracow University of Technology, Cracow, Poland

Corresponding Author: Robert Szczepanek
Email address: robert@szczepanek.pl

At the turn of February and March 2020, COVID-19 pandemic reached Europe. Many countries, including Poland imposed lockdown as a method of securing social distance between potentially infected. Stay-at-home orders and movement control within public space not only affected the tourism industry, but also the everyday life of the inhabitants. Hourly time-lapse from four HD webcams in Cracow (Poland) are used in this study to estimate how pedestrian activity changed during COVID-19 lockdown. The collected data cover the period from June 9, 2016 to April 19, 2020 and come from various urban zones. One zone is tourist, one is residential, and two are mixed. At the first stage of the analysis, state-of-the-art machine learning algorithm (YOLOv3) is used to detect people. Splitting the HD image into smaller tiles increases the number of detected pedestrians by over 50%. A non-standard application of the YOLO method, oriented on images from HD webcams, is proposed. This approach (YOLO tiled) is less prone to pedestrian detection errors, and the only disadvantage is the longer computation time. In the second stage, pedestrian activity analysis before and during the COVID-19 lockdown is conducted for hourly, daily and weekly averages. Depending on the type of urban zone, the number of pedestrians decreased from 33% in residential zones to 85% in tourist zones located in the Old Town. This corresponds to the reference data published as Google COVID-19 Community Mobility Reports. The developed method is available in the form of Python scripts and jupyter notebooks in a public repository with an open source license. It allows detection and counting of pedestrians anywhere from HD time-lapse webcams. The created database with the detected hourly number of nine types of objects (including people, bicycles, cars, trucks) from the four-year observation period in Cracow is available as a result of this study.

1 Analysis of pedestrian activity before and 2 during COVID-19 lockdown, using webcam 3 time-lapse from Cracow and machine 4 learning.

5 Robert Szczepanek¹

6 ¹Faculty of Environmental and Power Engineering, Cracow University of Technology,
7 Poland

8 Corresponding author:

9 Robert Szczepanek, ul. Warszawska 24, 31-155 Cracow, Poland¹

10 Email address: robert.szczepanek@pk.edu.pl

11 ABSTRACT

12 At the turn of February and March 2020, COVID-19 pandemic reached Europe. Many countries, including
13 Poland imposed lockdown as a method of securing social distance between potentially infected. Stay-at-
14 home orders and movement control within public space not only affected the tourism industry, but also
15 the everyday life of the inhabitants. Hourly time-lapse from four HD webcams in Cracow (Poland) are
16 used in this study to estimate how pedestrian activity changed during COVID-19 lockdown. The collected
17 data cover the period from June 9, 2016 to April 19, 2020 and come from various urban zones. One
18 zone is tourist, one is residential, and two are mixed. At the first stage of the analysis, state-of-the-art
19 machine learning algorithm (YOLOv3) is used to detect people. Splitting the HD image into smaller tiles
20 increases the number of detected pedestrians by over 50%. A non-standard application of the YOLO
21 method, oriented on images from HD webcams, is proposed. This approach (YOLO _{tiled}) is less prone to
22 pedestrian detection errors, and the only disadvantage is the longer computation time. In the second
23 stage, pedestrian activity analysis before and during the COVID-19 lockdown is conducted for hourly,
24 daily and weekly averages. Depending on the type of urban zone, the number of pedestrians decreased
25 from 33% in residential zones to 85% in tourist zones located in the Old Town. This corresponds to the
26 reference data published as Google COVID-19 Community Mobility Reports. The developed method is
27 available in the form of Python scripts and jupyter notebooks in a public repository with an open source
28 license. It allows detection and counting of pedestrians anywhere from HD time-lapse webcams. The
29 created database with the detected hourly number of nine types of objects (including people, bicycles,
30 cars, trucks) from the four-year observation period in Cracow is available as a result of this study.

31 INTRODUCTION

32 The COVID-19 pandemic that appeared in Europe in early 2020 has a major impact on societies around
33 the world. The economic, social and environmental impact affect many citizens. Many countries have
34 introduced extraordinary restrictions related to transport and use of public spaces. The direct effect of this
35 situation is a significant decrease in the number of pedestrians in public space.

36 Cracow is one of the most popular tourist cities in Poland (Central Europe). It is also an academic
37 center with the oldest university in Poland, the Jagiellonian University founded in 1364 by Casimir the
38 Great. With 771,069 inhabitants in 2018 and a population density of 2,359 person/km² (Rozkrut, 2019),
39 Cracow is the second largest city in Poland. Being one of the oldest cities with many tourist attractions,
40 virtually all year round the center of the Old Town is visited by many tourists from home and abroad.

41 In Poland, the first case of COVID-19 was officially confirmed on March 4, 2020. On March 13,
42 2020, the Polish government announced the first restrictions related to COVID-19. This included limiting
43 the activities of shopping centers, restaurants, bars and cafes, closing swimming pools and gyms. A
44 significant reduction in mobility was introduced on March 24 (Jarynowski et al., 2020). The ban on

45 leaving home did not only include going to work, a store or a pharmacy. Additional restrictions on the
46 operation of markets were introduced on March 31.

47 Patterns of human activity in the urban environment depend on several factors, such as, for example,
48 night lighting (Wang et al., 2019), but the impact of formal restrictions on movement in public space is
49 rarely considered and analyzed. In addition to public video surveillance systems, there are also private
50 video monitoring systems that can also be used to detect and count people. Some of them have been
51 running continuously for several years, enabling comparative studies with pre-pandemic periods.

52 The study has two main goals: to evaluate the YOLOv3 people detection algorithm on images from
53 HD webcams and application of YOLOv3 to assess changes in pedestrian activity in public space before
54 and during COVID-19 lockdown in Cracow, based on the hourly webcam time-lapse.

55 **Social distance during COVID-19**

56 Wellenius et al. (2020) used anonymous and aggregated mobility data (Aktay et al., 2020) to assess social
57 distance in the United States during COVID-19. The impact of the social distance order was very different
58 in each state, from a 36% drop in displacement New Jersey to a 12% drop in Louisiana. The most effective
59 ban was to impose restrictions on the work of bars and restaurants, which was associated with a 25.8%
60 reduction in people's activity. Wellenius et al. (2020) concludes that public procurement seems to be
61 very effective in encouraging people to stay at home to minimize the risk of COVID-19 transmission.
62 In the case of Poland, in COVID-19 Community Mobility Report (March 29, 2020), mobility trends in
63 places such as restaurants, cafes, shopping centers, theme parks and museums fell by 78%. In the case
64 of the Lesser Poland Voivodship in which Cracow is located, this decrease is 84% (Aktay et al., 2020).
65 Social behavior has a fundamental impact on the dynamics of the spread of infectious diseases (Prem
66 et al., 2017). Inhabitants of larger Polish cities are more afraid of overcrowded hospitals and inefficient
67 healthcare than small towns and villages (Jarynowski et al., 2020).

68 The Center for Science and Systems Engineering (CSSE) at Johns Hopkins University provides daily
69 data updates via COVID-19 Data Repository (Dong et al., 2020). The first confirmed cases of COVID-19
70 in Italy and Spain were identified at the end of February 2020 (Saglietto et al., 2020). The lockdown has
71 been widely used in Italy since March 8 and in Spain since March 16. Restrictions on citizens' mobility
72 have reduced disease transmission in both countries (Tobías, 2020).

73 Chinazzi et al. (2020) findings indicate that 90% of travel restrictions to and from mainland China only
74 modestly affect the epidemic trajectory unless combined with a 50% or higher reduction of transmission
75 in the community. Fang et al. (2020) uses the crowd flow model for virus transmission to simulate the
76 spread of the virus caused by close contact during pedestrian traffic. Mobility restrictions are important
77 (Arenas et al., 2020; Ferguson et al., 2020) or sometimes crucial (Mitjà et al., 2020), but as shown by
78 Mello (2020) the number of people crossing each other can be drastically reduced if one-way traffic is
79 enforced and runners are separated from walkers. To properly quantify the transmission of an epidemic,
80 the spatial distribution of potential disease hazards (e.g. crowd) should be assessed (Ng and Wen, 2019;
81 Fang et al., 2020). Webcams can be a potential source of such information.

82 **People detection**

83 Object detection is one of the rapidly growing areas of computer vision. Proper detection of people is
84 crucial for autonomous cars, advertising planning and many other industries and public safety. Kajabad
85 and Ivanov (2019) proposed a method of finding areas more attractive to customers (hot zones) based
86 on people detection. Sometimes, people must be detected in a heavy industry environment (Zengeler
87 et al., 2019) or in hazy weather (Li et al., 2019). A lot of research is being done to detect objects in a
88 variety of environments, but this is not just about detecting people. Computer vision methods are used to
89 count species in environmental research: 1 minute time-lapse for fish passage and abundance in streams
90 (Deacy et al., 2016), or 5 minute time-lapse for bears counting (Deacy et al., 2019). There are two main
91 approaches to detecting a person or other object in the image. The first approach is based on computer
92 vision techniques, the second on deep learning algorithms.

93 **Computer vision**

94 Traditional pedestrian detectors have been known for over two decades. They are based on the repre-
95 sentation of the features of objects obtained from computer vision. Oren et al. (1997) proposed the use
96 of Haar waves in 1997, and Maliniowski in 2005 the use of the Oriented Gradient (HOG) Histogram.
97 Also Local Binary Patterns (LBP) (Ojala et al., 2002) can be used for pedestrian detection (Zheng et al.,

2010). Among them, HOG and its variations are considered the most successful hand-engineered features for pedestrian detection (Liu et al., 2016a, 2019b). For visual surveillance applications, background subtraction method can also be used (Maddalena and Petrosino, 2008). In hybrid implementation of computer vision methods, pedestrian detection on the basis of 2D/3D LiDAR data and visible images of the same scene are applied (Hasfura, 2016; El Ansari et al., 2018).

103 **Deep learning**

104 In recent years, several convolutional neural networks (CNN) models for object detection have been
105 proposed (Ren et al., 2018): R-CNN in 2014, Fast R-CNN in 2015 and Faster R-CNN in 2015. These
106 two-step detection algorithms divide the problem into two stages: (i) generating region proposals and (ii)
107 classification of candidate regions. But these traditional deep learning algorithms suffer from low speed
108 (Kajabad and Ivanov, 2019). To overcome this limitation, Redmon et al. (2016) proposed a one-step
109 detection algorithm called YOLO, enabling easy implementation end-to-end object detection. Further
110 improvements of this algorithm are known as YOLO9000 (or YOLOv2) (Redmon and Farhadi, 2017) and
111 YOLOv3 (Redmon and Farhadi, 2018). Second popular one-stage algorithms is RetinaNet (Lin et al.,
112 2017). It deals with the problem of the extreme foreground-background class imbalance encountered
113 during the training of dense detectors and proposes a new solution to this problem. Third detection
114 algorithm is Single Shot MultiBox Detector (SSD). The core of SSD is predicting category scores and
115 box offsets for a fixed set of default bounding boxes using small convolutional filters applied to feature
116 maps (Liu et al., 2016b). To improve model performance for small objects, SSD applies additional data
117 augmentation strategy. All three algorithms achieve state-of-the-art speed and accuracy (Zengeler et al.,
118 2019), so they can be used in real-time applications.

119 The original YOLO model trains the classifier network at 224×224 and increases the resolution to
120 448×448 for detection (Redmon and Farhadi, 2017). Backbone for YOLOv3 is Darknet-53 network, and
121 standard image sizes are 320×320 . YOLOv3 makes detection at three different scales downsampling the
122 dimensions of the input image by 32, 16, and 8. Darknet architecture is a pre-trained model for classifying
123 80 different classes. Several improvements to the YOLO model have been proposed for detecting people
124 (Putra et al., 2017, 2018; Lan et al., 2018; He et al., 2019; Li et al., 2019), but even standard YOLOv3
125 outperforms traditional computer vision methods and most of deep neural network methods (Ghosh and
126 Das, 2019; Zengeler et al., 2019; Kajabad and Ivanov, 2019; Yun et al., 2018). Pre-trained networks for
127 standard image sizes are available in several repositories, enabling fast and relatively easy application of
128 YOLO model. Squeeze YOLO-based People Counting (S-YOLO-PC) proposed by Ren et al. (2018) can
129 detect and count people with 41 frames per second (FPS) with the Average Precision (AP) of 72%. Feng
130 et al. (2019) reports YOLOv2 mean Average Precision (mAP) of 76.8%, which is very close to 78.6%
131 reported by authors of YOLO method (Redmon and Farhadi, 2017). However, even the latest version of
132 YOLOv3 has some limitations. If there are two anchor boxes but three objects in the same grid cell, it
133 does not support them correctly, which ultimately leads to missing objects (Kajabad and Ivanov, 2019).
134 YOLO achieves about 10% missing detection rate for pedestrian detection (Lan et al., 2018). Yun et al.
135 (2018) reports that YOLOv3 default architecture achieves the mAP of 42.7%.

136 **Object size and crowd counting**

137 Robustly detecting pedestrians with a large variant on sizes and with occlusions remains a challenging
138 problem (Liu et al., 2019a,b). Pedestrian detection is limited by image resolution and complexity of
139 the background scene. Effective detector should be able to detect people at different scales. Liu et al.
140 (2018) presents a method where a large-size pedestrian should be represented by features from deep
141 layers, whereas a small-size pedestrian should be represented by features from shallow layers which
142 are of higher resolutions. Liu et al. (2019a) propose gated feature extraction framework consisting of
143 squeeze units, gate units and a concatenation layer which perform feature dimension squeezing, feature
144 elements manipulation and convolutional features combination from multiple CNN layers. Evaluation of
145 average precision and the tuning of the model is usually limited to objects in the 50-100 m range, as in the
146 CityScapes Dataset for Semantic Urban Scene Understanding (Cordts et al., 2016).

147 Next issue in urban space or during mass events is the crowd. There are mainly three types of methods
148 to count the number of people in the crowd from video (Ren et al., 2018): (i) statistical method to estimate
149 the number of people in a region, (ii) combination of object detection with object tracking and (iii) use of
150 path information of the points, with subsequent cluster analysis of the feature point path. People detection
151 in crowded spaces is the most challenging task, because of the people occlusions (Stewart et al., 2016;

152 Kajabad and Ivanov, 2019). Crowd counting requires development of new methods (Stewart et al., 2016;
 153 Lei et al., 2020) like Dynamic Region Division (He et al., 2019). Existing crowd counting methods require
 154 object location-level annotation or weaker annotations that only know the total count of objects (Lei et al.,
 155 2020).

156 Only the problem of the size of the object (person) is examined in the first part of these studies. Due
 157 to the convenient location of the webcam (between the first and sixth floors) and low to moderate density
 158 of pedestrians, crowd counting methods can be omitted.

159 MATERIALS & METHODS

160 Study area

161 Images from webcams are collected in Cracow, the second largest city in the country and the capital of
 162 the Lesser Poland Voivodeship. Cracow is divided into the medieval Old Town, located in the center and
 163 the surrounding residential and industrial zones. The Vistula, the largest river in Poland, flows through the
 164 city center.

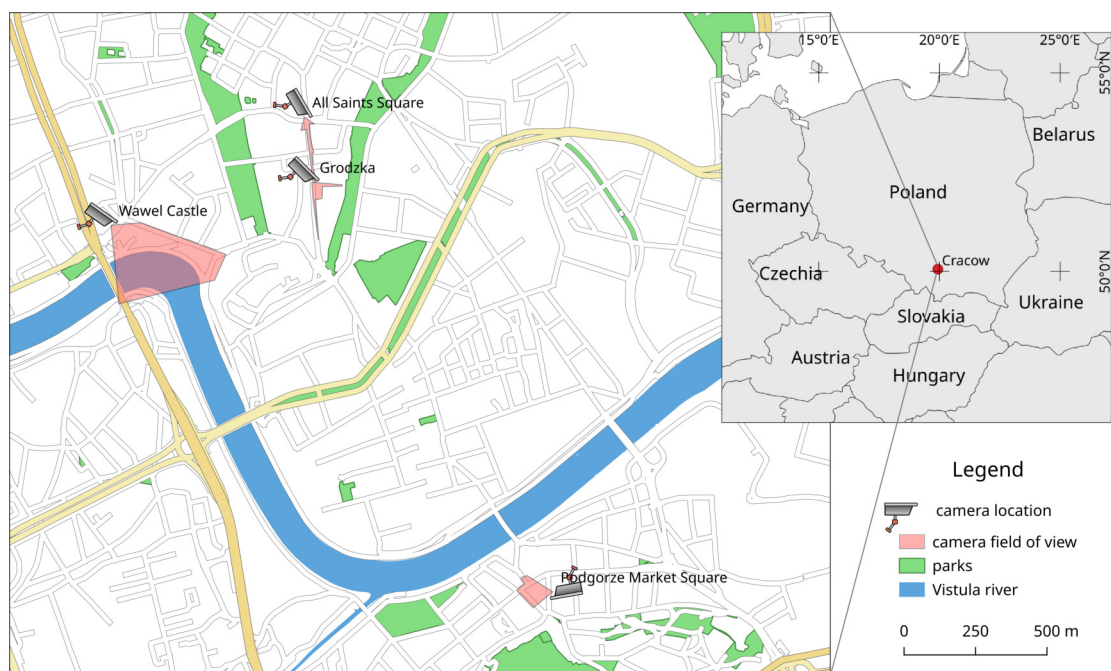


Figure 1. Location in Cracow (Poland) and approximate field of view for webcams used in these studies (www.webcamera.pl). Technical details in Table 1.

165 Two of the webcams are located on the Royal Road, going from Wawel Castle through Main Square to
 166 north of the city. These webcams are named All Saints Square and Grodzka (Fig. 1). Grodzka Street has
 167 a tourist character, and All Saints Square, being in the tourist zone, is also an important communication
 168 point in the city (Tab. 1). The third webcam (Wawel Castle) is located in the tourist/residential zone.
 169 Parking for tourists visiting Wawel Royal Castle is adjacent to the riverside promenade, which is used by
 170 residents. The fourth webcam (Podgorze Market Square) is a typical residential zone located on the other
 171 side of the Vistula river (Fig. 1).

172 Due to the medieval nature of the area, cameras from Royal Road have a very narrow field of view.
 173 The webcam on All Saints Square is located on a small square, so in fact most of the visible pedestrian
 174 area belongs to Grodzka Street. This webcam is also in the lowest position among all four, enabling easier
 175 detection of pedestrians due to the short distance from the detected objects. The Wawel Castle webcam
 176 with probably the most beautiful view from all Cracow webcams has the largest distance to detected
 177 pedestrians and is the highest mounted webcam (the sixth floor).

178 All webcams are publicly available and broadcast live via dedicated websites (Tab. 1), but access to
 179 the ad-free version is limited due to the commercial nature of the service. Webcamera.pl is probably one

Webcam name	Distance to pedestrians (m)	Pedestrians area (ha)	Urban zone / URL
Wawel Castle	50–400	0.92	touristic / residential https://krakow2.webcamera.pl/
All Saints Square	10–150	0.32	touristic mainly https://krakow1.webcamera.pl/
Grodzka	10–100	0.14	touristic https://hotel-senacki-krakow.webcamera.pl/
Podgorze Market Square	30–120	0.31	residential https://krakow3.webcamera.pl/

Table 1. Webcam visibility range and source image URLs. Pedestrians area refers to the part of the area accessible to pedestrians.

180 of the largest providers of streaming cameras in Poland, with a long history and almost 350 webcams
 181 located all over Poland. To make detection results comparable, webcams with a moving field of view
 182 were excluded from the analysis, although they are in very good locations, such as the Main Square, the
 183 largest medieval town square in Europe (<https://krakow4.webcamera.pl/>).

184 Webcam time-lapse

185 Webcam time-lapse is made and downloaded every hour (Fig. 2), directly from www.webcamera.pl
 186 provider. In this study, approximately 33,800 images were collected and used for each webcam from June
 187 9, 2016 to April 19, 2020. The analysis is based on 1,412 days (201 weeks) of continuous observation.
 188 The total size of the set of hourly time-lapse images for four webcams in this period exceeds 10 GB.

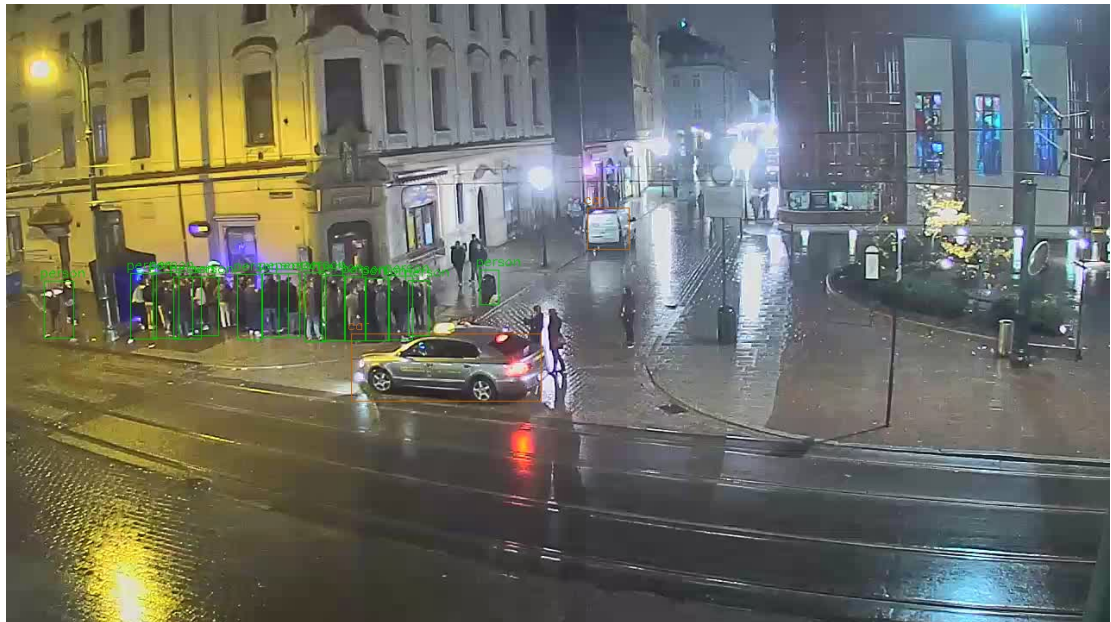


Figure 2. Sample image from All Saints Square webcam at midnight, with pedestrians and cars detected by YOLO. Timestamp: 2016-10-29 00:00.

189 Methods

190 The standard Darknet-53 architecture with the YOLOv3 model is used as the main pedestrian detector.
 191 The interface to the model is built in the Python 3 programming language, in the main script `yolo_count.py`.
 192 All code is available in the public repository (<https://gitlab.com/Cracert/pedestrian-count-covid-19>) under
 193 the MIT license. The OpenCV library (Bradski, 2000) with built-in support for the Darknet architecture is
 194 used in these studies as a machine learning platform. From the pre-trained Darknet architecture, only the

195 first 9 classes (from 80) are saved during calculations. These classes (person, bicycle, car, motorcycle,
 196 airplane, bus, train, truck, boat) are directly related to the urban space and can be used for other research.
 197 The results of pedestrian detection are counted and saved in CSV files for each year of the webcam, with
 198 one row corresponding to one hour.



Figure 3. The upper left two tiles from the split image (Fig. 2). Pedestrians (A) undetected and (B) detected by $YOLO_{tiled}$ method.

199 The pre-trained YOLOv3 model weights for people detection are available for direct use, so the
 200 training phase can be omitted (<https://pjreddie.com/media/files/yolov3.weights>). One of the standard
 201 image resolutions for training is 416×416 , while the source HD webcam image resolution used in this
 202 study is 1280×720 . As a first approach, YOLOv3 is applied directly to the collected images (Fig. 2).
 203 The second approach assumes that the right image ratio can improve the average precision of the model.
 204 The input images are divided into 6 almost square tiles 426×360 (Fig. 3). This reduces the image ratio
 205 from 1.78 (Fig. 2) to 1.18 (Fig. 3AB) and makes the image's proportions more similar to the training
 206 data set. In addition, not all tiles contain pedestrian areas, so some tiles can be omitted in the calculation,
 207 which significantly reduces detection time. Number of detected pedestrians is saved in data folder as CSV
 208 files (webcam_name-year-method.csv). Each file contains a header with the main detected classes and
 209 data containing a timestamp (day and hour) with the corresponding number of detected objects. One row
 210 corresponds to one hour time-lapse. Further analysis and visualization takes place in Jupyter notebooks
 211 (analysis-method.ipynb, analysis-pedestrians.ipynb) using the pandas library. For the purposes of this
 212 article, the YOLOv3 method will be named YOLO from this place, and the method of splitting one HD
 213 webcam image into six tiles will be named $YOLO_{tiled}$.

214 The comparison of the YOLO and $YOLO_{tiled}$ methods is based on statistical analysis. The number
 215 of pedestrians detected from each time-lapse (hour) enables the identification of extreme and mean
 216 differences between the two methods. Cases of extreme differences are examined manually to find
 217 problems associated with each method. In addition, the sum of detected pedestrians for the webcam over
 218 the entire period is used to detect the overall relative difference between YOLO and $YOLO_{tiled}$. In the
 219 second part of the study, a better method was used to assess the change in pedestrian numbers before and
 220 during COVID-19.

221 The image data provider returns the last image, so if the webcam fails, the same last recorded image
 222 is returned, resulting in a constant number of pedestrians over time. By analyzing such anomalies, you
 223 can determine the dates of webcam malfunction. The verification of the source image data based on
 224 the pedestrian number change analysis can be replicated in the supplied Jupyter notebook (analysis-
 225 pedestrians.ipynb). Doubtful periods are excluded from further analysis.

226 The webcam observation time is divided into (i) before the COVID-19 period, June 9, 2016 – March
 227 13, 2020 (1,374 days / 196 weeks) and (ii) during the COVID-19 period, March 13, 2020 – April 19,
 228 2020 (38 days / 5 weeks). The number of detected pedestrians for these two periods is aggregated into
 229 days and weeks using mean values. This makes it easier to visualize trends and generalize results. The
 230 mean number of pedestrians from the hourly period before and during COVID-19 is used for the final
 231 evaluation. A change in this value corresponds to changes in pedestrian activity over time. It is assumed
 232 that hourly snapshots (time-lapse) from webcams are representative for evaluation of relative change in
 233 pedestrian activity. However, the method presented is not suitable for determining the absolute number of

234 pedestrians traveling through the analyzed area.

235 RESULTS

236 The first part of the research focuses on assessing the YOLO pedestrian detection method and comparing
237 with $YOLO_{tiled}$. The number of detected pedestrians (people) for each hourly image from four webcams
238 in Cracow from 2016–2020 is saved for YOLO and $YOLO_{tiled}$ method.

239 On average, YOLO results are underestimated compared to the $YOLO_{tiled}$ method. Webcams located
240 at Royal Road (All Saints Square and Grodzka) had the highest absolute detected pedestrian differences up
241 to 50 person (Tab. 2). The other two webcams, located in the residential and mixed zone, had differences
242 of less than 25 people.

	Webcam			
	Wawel Castle	All Saints Square	Grodzka	Podgorze Market Square
$\max(YOLO_{tiled} - YOLO)$	15	50	49	24
$\text{mean}(YOLO_{tiled} - YOLO)$	0.36	5.70	4.43	0.33
$\max(YOLO - YOLO_{tiled})$	12	12	5	7
$\max(YOLO_{tiled})$	16	80	58	34
$\text{mean}(YOLO_{tiled})$	0.5	16.6	7.0	0.9
$\text{sum}(YOLO)$	4,064	369,497	86,538	17,642
$\text{sum}(YOLO_{tiled})$	16,367	562,122	236,252	28,749
Detection difference (%)	+302	+52	+173	+62.96

Table 2. Statistics of detected pedestrian number by YOLO and $YOLO_{tiled}$ method.

243 The mean number of detected pedestrians per image $\text{mean}(YOLO_{tiled})$ depends on the type of urban
244 zone, with 16.6 pedestrians in the tourist zone and 0.9 pedestrians in the residential zone (Tab. 2). The
245 mean difference of detected pedestrians between the two methods is the same, with values exceeding 4.4
246 in the tourist zone and below 0.4 in the residential zone.

247 Opposite cases are also reported when $YOLO_{tiled}$ detects fewer pedestrians, but in this case the absolute
248 difference does not exceed 12 pedestrians (Tab. 2). The maximum number of detected pedestrians also
249 corresponds to the location of the webcam. Tourist locations in the Old Town (All Saints Square and
250 Grodzka) record up to 80 pedestrians in one image (Fig. 4), and in residential zones below 35 (Tab.
251 2). Simply cutting one large image (Fig. 4A) into six smaller tiles (Fig. 4B) significantly increases the
252 number of correctly detected pedestrians. The detection range also increases, but a certain pedestrian
253 detection threshold is clearly visible at the horizontal cutting height of the tiles.



Figure 4. Pedestrian detection from All Saints Square webcam by (A) YOLO and (B) $YOLO_{tiled}$ method. Both views are framed to the central part. $YOLO_{tiled}$ view without the upper left tile.

254 The total sum of detected pedestrians over the entire period (almost 4 years) is from about 4,000 for
255 YOLO from Wawel Castle webcam to over 500,000 for $YOLO_{tiled}$ from All Saints Square. The relative

256 detection differences between YOLO and YOLO_{tiled} are significant and range from 52% on All Saints
 257 Square to 302% at Wawel Castle. This difference is proportional to the mean distance from pedestrians
 258 (Tab. 1).

259 Over long distances YOLO_{tiled} can detect significantly more pedestrian than YOLO. An example of
 260 such a case is shown on results from All Saints Square (Fig. 4) and from Wawel Castle webcam (Fig. 5).
 261 Wawel Castle webcam has the longest distance from pedestrians, from about 50 m to about 400 m. Also
 262 in this case, the detection range of pedestrians does not exceed about 200 m. Pedestrians in Figure 5C,
 263 near the detected boat at the upper part, are also not recognized.

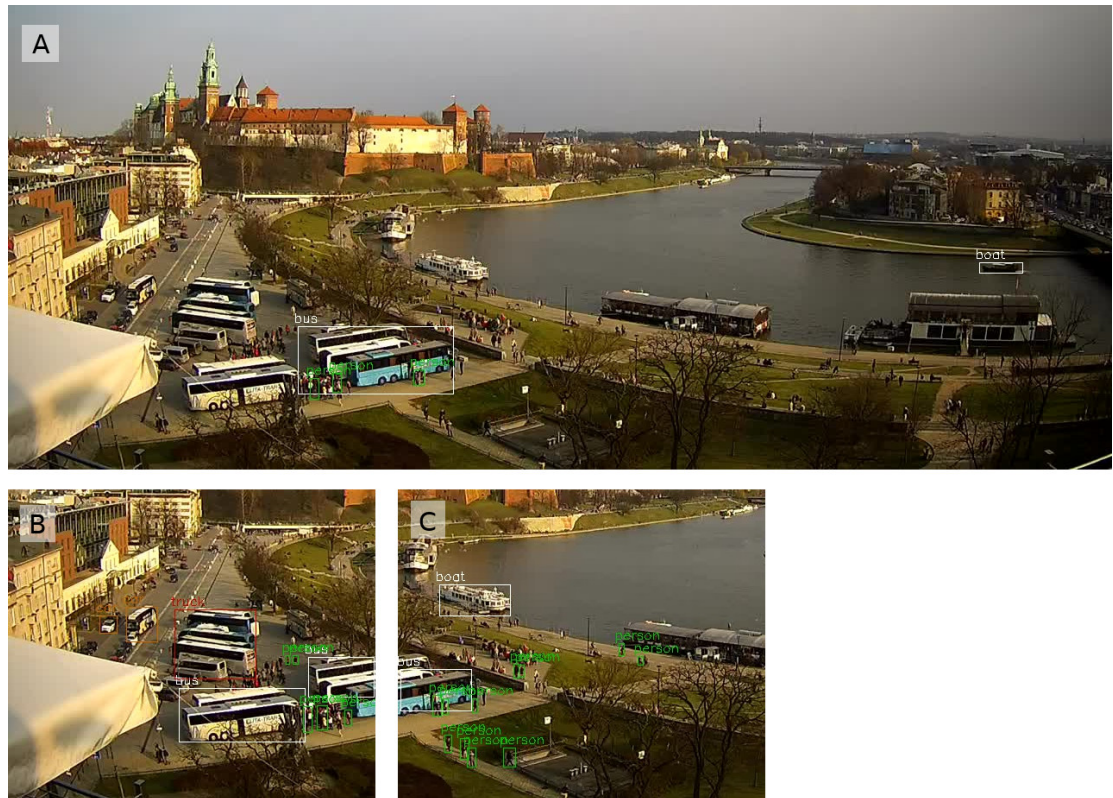


Figure 5. The biggest difference from the Wawel webcam, with more pedestrians detected by YOLO_{tiled} method. Results from (A) YOLO method, and (B)(C) two bottom left tiles from YOLO_{tiled} method.

264 The histogram of the difference in pedestrian detection $YOLO_{tiled} - YOLO$ is asymmetrical (Fig. 6).
 265 This also applies to other webcams. The difference of zero is dominant for all webcams, but mean value
 266 of 5.70 for the All Saints Square camera compared to the extreme number of detected pedestrians on one
 267 image in the range of 50–80 (Tab. 2) makes this difference significant. As a result, the YOLO_{tiled} method
 268 is selected as a better representation of the actual number of pedestrians on webcam time-lapse. With
 269 the awareness that this value is also underestimated in relation to the actual number of pedestrians on
 270 one image. Assuming that the detection range for both methods is constant (YOLO and YOLO_{tiled}), this
 271 should not significantly affect the estimation of the relative change in the number of pedestrians.

272 The YOLO_{tiled} method, which is a better detector, is used as the basis for the second part of research
 273 related to estimating pedestrian activity before and during COVID-19. Data analysis enabled the iden-
 274 tification of periods during which camera malfunction or camera data transmission was highly likely.
 275 These periods were removed from the dataframe and treated as no data. A detailed analysis with relevant
 276 comments can be found in analysis-pedestrians.ipynb Jupyter notebook. A few short periods have been
 277 removed from the dataframe for All Saints Square and Grodzka webcams (Fig. 7A). Another problem
 278 was identified in Podgorze Market Square, where two periods are characterized by significantly different
 279 average values of detected pedestrians. It was found that in mid-2019 the horizontal angle of the webcam
 280 was changed, which changed the field of view. In order to maintain the possibility of comparison with the
 281 current period (COVID-19), it was decided to abandon the first part of the dataframe (Fig. 7B).

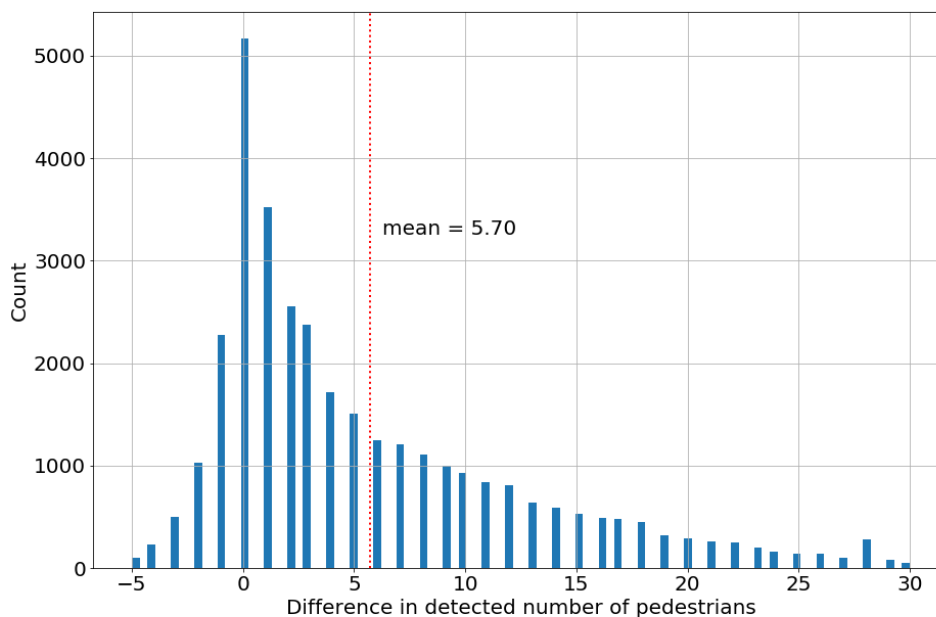


Figure 6. The difference in the number of pedestrians detected ($YOLO_{tiled} - YOLO$) for All Saints Square webcam.

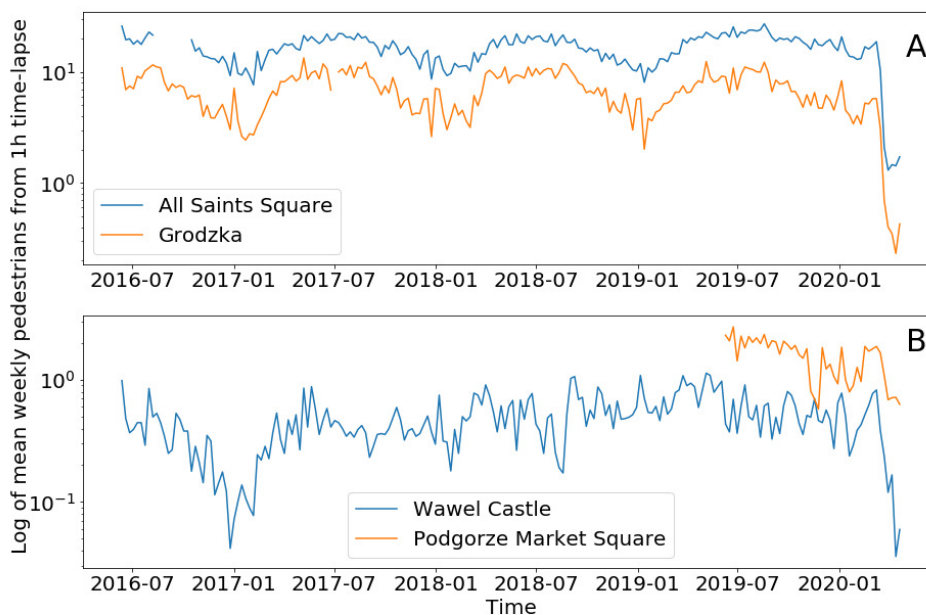


Figure 7. Mean weekly number of pedestrians from hourly time-lapse for (A) two tourist locations and (B) two residential (mixed) locations. Logarithmic scale on both plots for better visualization of annual cycles in tourist locations.

282 The high temporal variability of hourly data makes it difficult to visualize the result. For this reason,
283 daily and weekly data aggregation is used for visual analysis.

284 On the mean weekly plot, the seasonal cycle in the tourist zone is clearly visible (Fig. 7A) and is
285 associated with the summer season. In a residential zone, this seasonal cycle is not visible (Fig. 7B). In
286 the tourist zone, the mean number of pedestrians does not fall below one person per image (logarithmic
287 scale in Fig. 7), while in the residential zone the level is lower by an order of magnitude. There are
288 no visible trends in the number of pedestrians during these four years, but the COVID-19 lockdown is
289 clearly visible in the last weeks of the analyzed period (Fig. 7). The quantitative analysis of this change
290 is presented in the Table 3. Data from the Wawel Castel webcam are more difficult to interpret due to
291 the large distance from pedestrians, which results in a very low detection rate. Therefore, data from
292 this webcam is underestimated and caution should be exercised. Also the results from Podgorze Market
293 Square are difficult to interpret due to the relatively short period of homogeneous observations.

294 A quantitative analysis of pedestrian activity before and during COVID-19 from four locations in
295 Cracow is shown in the Table 3.

	Webcam			
	Wawel Castle	All Saints Square	Grodzka	Podgorze Market Square
Before COVID-19	0.49	16.86	7.13	1.66
During COVID-19	0.14	2.04	0.57	0.82
Change (%)	-54.64	-78.41	-85.32	-33.82

Table 3. Mean number of pedestrians detected by YOLO_{tiled} method from hourly time-lapse, before and during COVID-19.

296 Before COVID-19, the All Saint Square webcam registered about ten times as many pedestrians
297 compared to Podgorze Market Square (Fig. 3). During COVID-19 this ratio changed to 2:1. The largest
298 decrease in the number of pedestrians (85%) is observed on the Grodzka camera, which is a typical tourist
299 destination, and the lowest on Podgorze Market Square (34%) in the residential zone. Mixed urban zones,
300 with tourist and residential activities, report a moderate decrease in pedestrian numbers, from 55% to
301 78%. About 1,000 hourly time-lapse images during COVID-19 and 33,000 images before this period for
302 each webcam is a long enough time series to draw final conclusions.

303 DISCUSSION

304 Detection of pedestrians using the YOLO algorithm has good accuracy, but you can improve them by
305 simply adjusting the size of the webcam image to the size of the image used for neural network training.
306 The split of the original high resolution image into six smaller images increased the number of detected
307 pedestrians from 52.13% to 302.73% (Fig. 2). These values are proportional to the visible distance of the
308 webcam. At short distances (All Saints Square), mainly pedestrians near the camera are visible in the
309 field of view. In the case of large distances (Wawel Castle), where the nearest pedestrian is visible at a
310 distance of 100 m, split of images into smaller tiles causes a significant change in the number of detected
311 pedestrians. The cost of better results using the YOLO_{tiled} method is a longer calculation time.

312 On the other hand, in crowded scenes, the standard YOLO method works much better than YOLO_{tiled}.
313 This is visible when comparing Figure 2 with Figure 3A, or Figure 8C with Figure 8D and Figure 8E.

314 Differences in the number of pedestrians detected (Tab. 2, Fig. 6) are often caused by errors related to
315 incorrect classification of objects. Trashcans from Grodzka webcam (Fig. 8A) or advertisements from
316 Podgorze Market Square (Fig. 5B) are recognized by YOLO as persons. The same problem is visible in
317 Figure 2, where the objects detected by YOLO as people (on the extreme left and right) are actually trash
318 containers. A potential problem with YOLO_{tiled} may be double detection of a large object (e.g. bus) split
319 into two tiles. But for pedestrians, this issue is negligible.

320 The practical range of pedestrian detection with YOLO can be slightly improved using the tiled
321 method, but it is still limited to about 200 m. Beyond this distance, pedestrians are simply too small to be
322 detected. The problem that is difficult to solve with both YOLO and YOLO_{tiled} is the crowd. Methods
323 based on the YOLO algorithm are not oriented to detect people in crowded scenes.

324 The Figure 9 is the best illustration of changes in pedestrian activity in Cracow before and during
325 COVID-19. Five weeks during lockdown (from the First restrictions) and a few weeks earlier show how



Figure 8. The biggest difference in pedestrian detection for three webcams – less pedestrians from YOLO_{tilde} method. Error assigning class: (A) trashcan from Grodzka (bottom right), (B) advertisement display from Podgorze (only one real person was detected). Better detection of people in crowd from Wawel webcam (C) by YOLO compared to (D)(E) YOLO_{tilde} method.

326 significant was the decrease in pedestrian activity in public space. Subsequent restrictions (second and
 327 third) did not change the situation. Weekly cycles visible in almost all locations are replaced by flat lines
 328 since the first restrictions in mid-March. Until the end of the period under review, this trend remains
 329 unchanged.

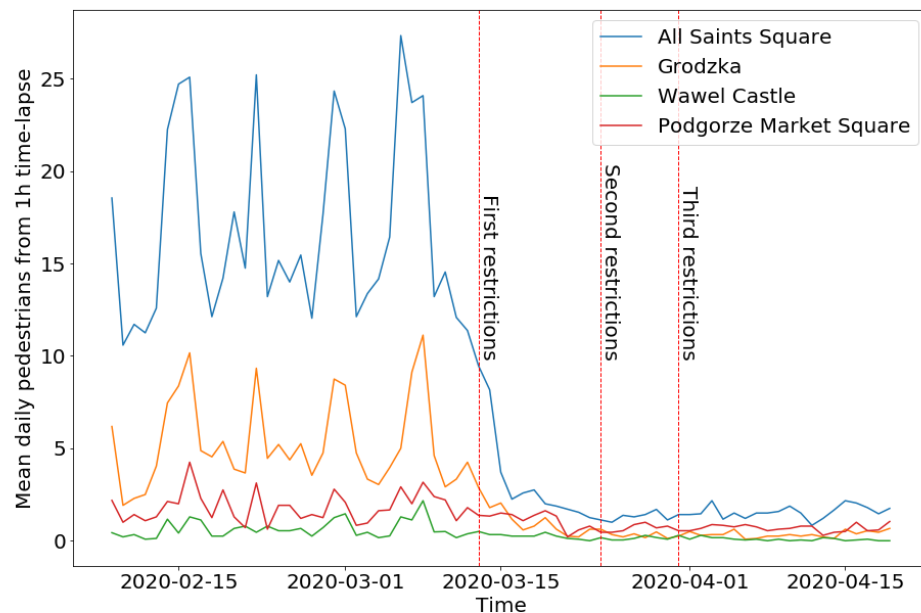


Figure 9. Mean daily number of pedestrians from hourly time-lapse for four webcams in Cracow, before and during COVID-19. Split time is set on First restrictions (2020-03-13).

330 During COVID-19, pedestrian activity in public spaces fell almost to zero. Observed values changed
 331 proportionally, except for two webcams. The number of detected pedestrians from the Grodzka webcam
 332 became smaller than the number of pedestrians from Podgorze Market Square (Fig. 9). This can be
 333 explained by a completely different nature of the location (urban zone). Grodzka street is occupied mainly
 334 by tourists, while Podgorze Market Square is mainly occupied by residents. This example shows the
 335 impact of COVID-19 on the tourism industry in Cracow. Reduced pedestrian mobility slows down the
 336 spread of COVID-19, but even temporary lockdown immediately affects the local community and local

337 economy. The first demonstrations of entrepreneurs against the lockdown began in Poland on May 7,
338 2020.

339 Wellenius et al. (2020) reports that the median of changes in time spent away from from places of
340 residence decreased by 19%. At the time of writing this article, only one quantitative assessment of
341 mobility trends for Poland during COVID-19 was available. As reported by Aktay et al. (2020) in Google
342 COVID-19 Community Mobility Reports for Poland (March 29, 2020), mobility trends for places like
343 restaurants, cafes, shopping centers, theme parks and museums decreased in Lesser Poland Voivodeship
344 (with Cracow) by 84%. This corresponds to the results from Grodzka and All Saints Square webcams,
345 with a reduced number of pedestrians by 85% and 78%, respectively (Tab. 3). According Aktay et al.
346 (2020) mobility trends for workplaces in Cracow decreased by 41%. This corresponds to Podgorze Market
347 Square webcam with a 34% decrease (Tab. 3). The results from mobile applications developed by Google
348 and presented in this analysis using machine learning and computer vision are very similar, despite the
349 use of completely different methods and approaches.

350 The overall results of the presented analysis are strongly influenced by the location of the webcam.
351 Two aspects are important: the urban zone, which determines the type of pedestrian (tourists or residents)
352 and the physical location of the webcam. There are mainly tourists on Grodzka Street. On All Saints
353 Square, most tourists mix with the locals. This is one of the key points within Old Town in Cracow with
354 City Hall located nearby. Wawel Castle webcam has similar (mixed) proportions of tourists to residents
355 as All Saints Square. On Podgorze Market Square tourists are rare guests. If the webcam is mounted low
356 (All Saints Square), the number of correctly detected pedestrians is very high. For webcams mounted
357 on top floors (Wawel Castle) or on roof of the building (Podgorze Market Square) chance of pedestrians
358 detection drop significantly. Another aspect of the physical location of the webcam is distance from
359 pedestrians. YOLO detectors are trained to detect objects on several scales, but too large a distance from
360 the object (Wawel Castle, Podgorze Market Square) makes it impossible to identify objects, including
361 pedestrians. For this reason, even split of HD webcam image into smaller tiles improves the accuracy of
362 the detector, but is also limited to about 200 m.

363 The properties of the YOLO detector probably allow the assessment of social distance between
364 pedestrians, which may be the next stage of data analysis. By applying a depth map and pedestrian
365 bounding boxes, it could be possible to quantify the social distances from the webcam image. In addition,
366 the goal-oriented tool can mask pedestrian areas, ignoring the others and thus reducing the calculation
367 time.

368 CONCLUSIONS

369 Detection of pedestrians in urban space can be done using the YOLOv3 method and hourly time-lapse
370 from webcams. A simple split of the HD webcam image into six smaller tiles in the proposed $YOLO_{\text{tiled}}$
371 method can increase the number of detected pedestrians by over 50%. The $YOLO_{\text{tiled}}$ method increases
372 the range of pedestrian detection compared to the YOLO method, but only up to a distance estimated in
373 this study at about 200 m. Pedestrians are not detected at longer distances.

374 During the COVID-19 pandemic lockdown in Cracow, from March 13, 2020 to April 19, 2020,
375 pedestrian activity decreased by 78-85% in the tourist zone (Old Town) and by 34-55% in the residential
376 zone. The results are very similar to the Google COVID-19 Community Mobility Reports, despite the use
377 of various methods. Polish citizens quickly and responsibly reacted to restrictions related to the social
378 distance, the visible manifestation of which was the limitation of pedestrian traffic in urban space during
379 the COVID-19 pandemic.

380 Developed as part of the work, the simple $YOLO_{\text{tiled}}$ method is available as open source code in
381 a public repository. Published code contains a full set of functions for tiling, detection and pedestrian
382 counting. The resulting hourly data with the number of people (pedestrians) for four webcams in Cracow
383 from June 9, 2016 to April 19, 2020 are available for further use as CSV files.

384 ACKNOWLEDGMENTS

385 The author would like to thank owners of www.webcamera.pl portal for providing access to HD webcams
386 in Cracow used in this research.

387 REFERENCES

- 388 Aktay, A., Bavadekar, S., Cossoul, G., Davis, J., Desfontaines, D., Fabrikant, A., Gabrilovich, E.,
389 Gadepalli, K., Gipson, B., Guevara, M., et al. (2020). Google COVID-19 Community Mobility Reports:
390 Anonymization Process Description (version 1.0). *arXiv preprint arXiv:2004.04145*.
- 391 Arenas, A., Cota, W., Gomez-Gardenes, J., Gomez, S., Granell, C., Matamalas, J. T., Soriano-Panos, D.,
392 and Steinegger, B. (2020). Derivation of the effective reproduction number R for COVID-19 in relation
393 to mobility restrictions and confinement. *medRxiv*.
- 394 Bradski, G. (2000). The OpenCV Library. *Dr. Dobb's Journal of Software Tools*.
- 395 Chinazzi, M., Davis, J. T., Ajelli, M., Gioannini, C., Litvinova, M., Merler, S., y Piontti, A. P., Mu,
396 K., Rossi, L., Sun, K., et al. (2020). The effect of travel restrictions on the spread of the 2019 novel
397 coronavirus (COVID-19) outbreak. *Science*, 368(6489):395–400.
- 398 Cordts, M., Omran, M., Ramos, S., Rehfeld, T., Enzweiler, M., Benenson, R., Franke, U., Roth, S., and
399 Schiele, B. (2016). The Cityscapes Dataset for Semantic Urban Scene Understanding. In *Proc. of the*
400 *IEEE Conference on Computer Vision and Pattern Recognition (CVPR)*.
- 401 Deacy, W. W., Leacock, W. B., Eby, L. A., and Stanford, J. A. (2016). A time-lapse photography method
402 for monitoring salmon (*Oncorhynchus* spp.) passage and abundance in streams. *PeerJ*, 4:e2120.
- 403 Deacy, W. W., Leacock, W. B., Stanford, J. A., and Armstrong, J. B. (2019). Variation in spawning
404 phenology within salmon populations influences landscape-level patterns of brown bear activity.
405 *Ecosphere*, 10(1):e02575.
- 406 Dong, E., Du, H., and Gardner, L. (2020). An interactive web-based dashboard to track COVID-19 in real
407 time. *The Lancet infectious diseases*.
- 408 El Ansari, M., Lahmyed, R., and Trémeau, A. (2018). A Hybrid Pedestrian Detection System based on
409 Visible Images and LIDAR Data. In *VISIGRAPP (5: VISAPP)*, pages 325–334.
- 410 Fang, Z., Huang, Z., Li, X., Zhang, J., Lv, W., Zhuang, L., Xu, X., and Huang, N. (2020). How many
411 infections of COVID-19 there will be in the "Diamond Princess"-Predicted by a virus transmission
412 model based on the simulation of crowd flow. *arXiv preprint arXiv:2002.10616*.
- 413 Feng, R.-C., Lin, D.-T., and Lin, Y.-Y. (2019). Multiple Objects Detection and Classification for Street
414 Intersection Surveillance Video Based on Deep Learning. Technical report, EasyChair.
- 415 Ferguson, N., Laydon, D., Nedjati-Gilani, G., Imai, N., Ainslie, K., Baguelin, M., Bhatia, S., Boonyasiri,
416 A., Cucunubá, Z., Cuomo-Dannenburg, G., et al. (2020). Impact of non-pharmaceutical interventions
417 (NPIs) to reduce COVID-19 mortality and healthcare demand. Imperial College COVID-19 Response
418 Team.
- 419 Ghosh, S. and Das, D. (2019). Comparative analysis and implementation of different human detection
420 techniques. In *2019 Fifth International Conference on Image Information Processing (ICIIP)*, pages
421 443–447. IEEE.
- 422 Hasfura, A. M. L. (2016). *Pedestrian detection and tracking for mobility on demand*. PhD thesis,
423 Massachusetts Institute of Technology.
- 424 He, G., Ma, Z., Huang, B., Sheng, B., and Yuan, Y. (2019). Dynamic region division for adaptive learning
425 pedestrian counting. In *2019 IEEE International Conference on Multimedia and Expo (ICME)*, pages
426 1120–1125. IEEE.
- 427 Jarynowski, A., Wójta-Kempa, M., Płatek, D., and Czopek, K. (2020). Attempt to understand public
428 health relevant social dimensions of COVID-19 outbreak in Poland. Available at SSRN 3570609.
- 429 Kajabad, E. N. and Ivanov, S. V. (2019). People detection and finding attractive areas by the use of
430 movement detection analysis and deep learning approach. *Procedia Computer Science*, 156:327–337.
- 431 Lan, W., Dang, J., Wang, Y., and Wang, S. (2018). Pedestrian detection based on YOLO network model.
432 In *2018 IEEE International Conference on Mechatronics and Automation (ICMA)*, pages 1547–1551.
433 IEEE.
- 434 Lei, Y., Liu, Y., Zhang, P., and Liu, L. (2020). Towards using count-level weak supervision for crowd
435 counting. *arXiv preprint arXiv:2003.00164*.
- 436 Li, G., Yang, Y., and Qu, X. (2019). Deep learning approaches on pedestrian detection in hazy weather.
437 *IEEE Transactions on Industrial Electronics*.
- 438 Lin, T.-Y., Goyal, P., Girshick, R., He, K., and Dollár, P. (2017). Focal loss for dense object detection. In
439 *Proceedings of the IEEE international conference on computer vision*, pages 2980–2988.
- 440 Liu, T., Elmikaty, M., and Stathaki, T. (2018). SAM-RCNN: Scale-Aware Multi-Resolution Multi-Channel
441 Pedestrian Detection. *arXiv preprint arXiv:1808.02246*.

- 442 Liu, T., Huang, J.-J., Dai, T., Ren, G., and Stathaki, T. (2019a). Gated Multi-layer Convolutional Feature
443 Extraction Network for Robust Pedestrian Detection. *arXiv preprint arXiv:1910.11761*.
- 444 Liu, T., Luo, W., Ma, L., Huang, J.-J., Stathaki, T., and Dai, T. (2019b). Coupled Network for Robust
445 Pedestrian Detection with Gated Multi-Layer Feature Extraction and Deformable Occlusion Handling.
446 *arXiv preprint arXiv:1912.08661*.
- 447 Liu, T.-R., Copin, V., and Stathaki, T. (2016a). Human Detection from Ground Truth Cameras through
448 Combined Use of Histogram of Oriented Gradients and Body Part Models. In *VISIGRAPP (4: VISAPP)*,
449 pages 735–740.
- 450 Liu, W., Anguelov, D., Erhan, D., Szegedy, C., Reed, S., Fu, C.-Y., and Berg, A. C. (2016b). SSD: Single
451 Shot MultiBox Detector. In *European conference on computer vision*, pages 21–37. Springer.
- 452 Maddalena, L. and Petrosino, A. (2008). A self-organizing approach to background subtraction for visual
453 surveillance applications. *IEEE Transactions on Image Processing*, 17(7):1168–1177.
- 454 Mello, B. A. (2020). Pedestrian traffic must be regulated in contagious epidemics. *arXiv preprint*
455 *arXiv:2004.00423*.
- 456 Mitjà, O., Arenas, À., Rodó, X., Tobias, A., Brew, J., and Benlloch, J. M. (2020). Experts' request to the
457 Spanish Government: move Spain towards complete lockdown. *The Lancet*.
- 458 Ng, T.-C. and Wen, T.-H. (2019). Spatially Adjusted time-varying Reproductive numbers: Understanding
459 the Geographical expansion of Urban Dengue outbreaks. *Scientific Reports*, 9(1):1–12.
- 460 Ojala, T., Pietikainen, M., and Maenpaa, T. (2002). Multiresolution gray-scale and rotation invariant
461 texture classification with local binary patterns. *IEEE Transactions on pattern analysis and machine*
462 *intelligence*, 24(7):971–987.
- 463 Oren, M., Papageorgiou, C., Sinha, P., Osuna, E., and Poggio, T. (1997). Pedestrian detection using
464 wavelet templates. In *Proceedings of IEEE computer society Conference on computer vision and*
465 *pattern recognition*, pages 193–199. IEEE.
- 466 Prem, K., Cook, A. R., and Jit, M. (2017). Projecting social contact matrices in 152 countries using
467 contact surveys and demographic data. *PLoS computational biology*, 13(9):e1005697.
- 468 Putra, M., Yussof, Z., Lim, K., and Salim, S. (2018). Convolutional neural network for person and car
469 detection using yolo framework. *Journal of Telecommunication, Electronic and Computer Engineering*
470 *(JTEC)*, 10(1-7):67–71.
- 471 Putra, M., Yussof, Z., Salim, S., and Lim, K. (2017). Convolutional neural network for person detection
472 using yolo framework. *Journal of Telecommunication, Electronic and Computer Engineering (JTEC)*,
473 9(2-13):1–5.
- 474 Redmon, J., Divvala, S., Girshick, R., and Farhadi, A. (2016). You only look once: Unified, real-time
475 object detection. In *Proceedings of the IEEE conference on computer vision and pattern recognition*,
476 pages 779–788.
- 477 Redmon, J. and Farhadi, A. (2017). YOLO9000: better, faster, stronger. In *Proceedings of the IEEE*
478 *conference on computer vision and pattern recognition*, pages 7263–7271.
- 479 Redmon, J. and Farhadi, A. (2018). YOLOv3: An incremental improvement. *arXiv preprint*
480 *arXiv:1804.02767*.
- 481 Ren, P., Wang, L., Fang, W., Song, S., and Djahel, S. (2018). A Novel Squeeze YOLO-based Real-time
482 People Counting Approach. *Int. J. of Bio-Inspired Computation*, 9(1):2.
- 483 Rozkrut, D., editor (2019). *Demographic Yearbook of Poland*. Statistics Poland, Warsaw.
- 484 Saglietto, A., D'Ascenzo, F., Zoccai, G. B., and De Ferrari, G. M. (2020). COVID-19 in Europe: the
485 Italian lesson. *The Lancet*, 395(10230):1110–1111.
- 486 Stewart, R., Andriluka, M., and Ng, A. Y. (2016). End-to-end people detection in crowded scenes. In
487 *Proceedings of the IEEE conference on computer vision and pattern recognition*, pages 2325–2333.
- 488 Tobías, A. (2020). Evaluation of the lockdowns for the SARS-CoV-2 epidemic in Italy and Spain after
489 one month follow up. *Science of The Total Environment*, page 138539.
- 490 Wang, D., Chen, J., Zhang, L., Sun, Z., Wang, X., Zhang, X., and Zhang, W. (2019). Establishing an
491 ecological security pattern for urban agglomeration, taking ecosystem services and human interference
492 factors into consideration. *PeerJ*, 7:e7306.
- 493 Wellenius, G. A., Vispute, S., Espinosa, V., Fabrikant, A., Tsai, T. C., Hennessy, J., Williams, B., Gadepalli,
494 K., Boulange, A., Pearce, A., et al. (2020). Impacts of State-Level Policies on Social Distancing in
495 the United States Using Aggregated Mobility Data during the COVID-19 Pandemic. *arXiv preprint*
496 *arXiv:2004.10172*.

- 497 Yun, Y., Park, Y., Woo, C., and Lim, S. (2018). Speed Accuracy Trade-off in Pedestrian and Vehicle
498 Detection Using Localized Big Data. In *2018 IEEE International Conference on Big Data (Big Data)*,
499 pages 1142–1149. IEEE.
- 500 Zengeler, N., Grimm, M., Borgmann, C., Jansen, M., Eimler, S., and Handmann, U. (2019). An Evaluation
501 of Human Detection Methods on Camera Images in Heavy Industry Environments. In *2019 14th IEEE
502 Conference on Industrial Electronics and Applications (ICIEA)*, pages 205–210. IEEE.
- 503 Zheng, Y., Shen, C., Hartley, R., and Huang, X. (2010). Effective pedestrian detection using center-
504 symmetric local binary/trinary patterns. *arXiv preprint arXiv:1009.0892*.